Biosourced Janus Molecules as Silica Coupling Agents in Elastomer Composites for Tires with Lower Environmental Impact

ACS Sustainable Chemistry & Engineering

pubs.acs.org/journal/ascecg

Research Article

Biosourced *Janus* Molecules as Silica Coupling Agents in Elastomer Composites for Tires with Lower Environmental Impact

Daniele Locatelli, Andrea Bernardi, Lucia Rita Rubino, Stefania Gallo, Alessandra Vitale, Roberta Bongiovanni, Vincenzina Barbera,* and Maurizio Galimberti*

Cite This: *ACS Sustainable Chem. Eng.* 2023, 11, 2713−2726

Read Online

ACCESS | Metrics & More | Article Recommendations | Supporting Information

ABSTRACT: A biosourced *Janus* molecule was used as a coupling agent between silica and unsaturated polymer chains in an elastomeric composite suitable for tire compounds with low energy dissipation, with potential important reduction of the environmental impact of the tire. 2-(2,5-Dimethyl-1*H*-pyrrol-1-yl)-1,3-propanediol (serinol pyrrole, SP) was synthesized through the neat reaction of serinol and 2,5-hexanedione, with a high atom efficiency (ca. 85%). Adducts of SP with silica were prepared (SP ≈ 9% by mass), with very high yield. In the whole process, from reagents to adducts, only substances from natural sources could be used, and the only co-product was water and the carbon efficiency was close to 100%. The silica/SP adduct was used in an elastomeric composite based on diene elastomers such as poly(styrene-co-butadiene) and poly(1,4-*cis*-isoprene) from *Hevea brasiliensis*. Comparison was made with a composite containing silica and a traditional coupling agent, a sulfur-based silane, bis(triethoxysilylpropyl)tetrasulfide (TESPT). SP appears to behave as a coupling agent for silica. To have similar properties for the SP and TESPT-based composites, tuning of the formulation of the composite with silica/SP has to be performed. Model reactions revealed the condensation of the OH of SP with the SiOR groups of an alkoxysilane, the reaction of the pyrrole ring with sulfur and a thiyl radical and the reaction of the sulfurated pyrrole ring with the unsaturation of squalene. SP appears thus able to establish covalent bonds with both silica and the unsaturated elastomer. With SP, the release of ethanol, which occurs from the silanization of silica with TESPT and is usually burned in industrial plants to give CO_2, is avoided. This work paves the way for the development at the industrial scale of elastomeric composites which allow remarkable reduction of the carbon footprint of the tire technology.

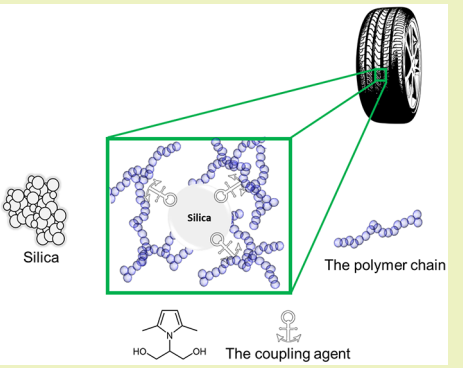

KEYWORDS: *rubber composites, pyrrole methodology, sulfur reactivity, silica functionalization, sustainability*

1. INTRODUCTION

Sustainability[1] is a "grand challenge"[2] for chemistry and engineering. The United States Environmental Protection Agency states that sustainability is "a guiding influence for all of our work".[3] To move people and things is a fundamental need of humanity and the role of transport in sustainable development is well recognized by the United Nations (UN)[4] since the 1992 United Nation's Earth Summit. Sustainable transport is integrated in several Sustainable Development Goals in the 2030 Agenda for Sustainable Development.[5] Numbers about mobility are indeed impressive. In 2016, global greenhouse emissions were 49.4 billion tonnes CO_2 equivalent.[6] Energy is the sector that most contributes to global greenhouse emissions (more than 70%) and road transport gives the highest contribution (about 12%). The Global Mobility Report 2017 of the UN[7] states that by 2030, annual passenger traffic and global freight volumes will grow by 50 and 70% with respect to 2015: 2.4 billion cars will be on the road.

The global market for tires is forecast to reach 2.7 billion units by 2025.[8] The contribution of tires to the carbon footprint of a car is reported to be about 20% and it is estimated[9] to be due to raw materials (6%), manufacturing (3%), distribution (0.2%), use (91%), and end of life (<0.1%). The environmental impact of a tire during its use essentially comes from the so-called rolling resistance (RR), which is defined as "the energy consumed per unit distance of travel as a tire rolls under load".[10] In order to reduce the RR of a tire, precipitated silica[11] is used as the reinforcing filler of tire compounds,[12−15] mainly for the tire tread but also and increasingly for other tire compounds. Silica has a polar surface, characterized by silanols and siloxane groups, and has a high surface area and activity. Compatibilization with the apolar hydrocarbon matrix, typical of a tire compound, is achieved by using the so-called coupling agents, which not only

Received: August 31, 2022
Revised: January 12, 2023
Published: February 6, 2023

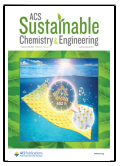

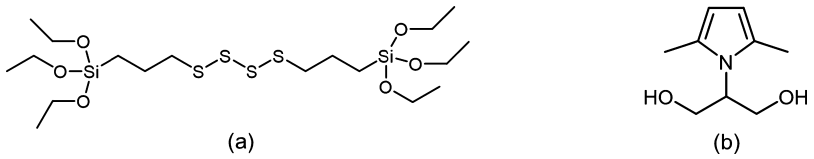

Figure 1. Chemical structure of (a) bis(triethoxysilylpropyl)tetrasulfide (TESPT) and (b) 2-(2,5-dimethyl-1*H*-pyrrol-1-yl)-1,3-propanediol (serinol pyrrole, SP).

shield the silica surface but also, and most of all, promote the formation of a chemical bond with the polymer chains.[13−15] The chemical link between the reinforcing filler and the elastomer matrix reduces the hysteresis of the compound and thus the dissipation of energy. The coupling agent, which is used also on an industrial scale, is a sulfur-containing silane: bis(triethoxysilylpropyl)tetrasulfide (TESPT). Its chemical structure is shown in Figure 1a.

The SiOR groups react with silica, during the compounding and cross-linking steps, and sulfur promotes the reaction with the polymer during cross-linking.[16,17] TESPT is an oil-based chemical. Moreover, it is widely acknowledged that the coupling reaction between TESPT and the elastomer chains has limited efficiency and the reaction of the SiOR groups of TESPT with silica releases one or two moles of ethanol for every silicon atom. It would thus be highly desirable to use, in rubber compounds for tires, a coupling agent alternative to TESPT, ideally a biosourced chemical,[18,19] whose reaction with the silanols on the silica surface could be in line with the principles of green chemistry,[20,21] showing a very high carbon efficiency. To act as a coupling agent, such a chemical should be reactive with the sulfur-based system used in vulcanization.

In this work, an alternative coupling agent between silica and the elastomer chains was used: 2-(2,5-dimethyl-1*H*-pyrrol-1-yl)-1,3-propanediol (serinol pyrrole, SP). Its chemical structure is shown in Figure 1b. SP has two moieties with different chemical reactivities, the aromatic pyrrole ring and the glycerol moiety bearing OH groups, which are supposed to be reactive with the sulfur/sulfur-based chemicals and with the silanols, respectively. SP is a glycerol derivative, obtained from the Paal Knorr reaction[22−24] of 2-amino-1,3-propandiol (serinol) with 2,5-hexanedione. Glycerol is an important co-product of biodiesel production,[25] which is one of the 15 selected structures that could be produced from a biorefinery[26,27] and can be converted to value-added products through different routes,[28] and serinol can be obtained from renewable sources as well.[29] Also 2,5-hexanedione can be prepared from a biobased chemical such as 2,5-dimethylfuran.[30−32] SP can thus be considered a biosourced *Janus* molecule.[33,34]

With SP as a coupling agent, ethanol emission would be avoided completely and high efficiency of the reaction with silica should lead to high carbon efficiency. Recently, it has been reported[35] that precipitated silica has excellent greenness scores when compared to higher value silicas such as the mesoporous ones. Hence, to improve the greenness of the silica functionalization reaction would be of great relevance.

Silica adducts with pyrrole derivatives were reported in the literature.[36−38] Silica−polypyrrole hybrids, prepared through the electrodeposition method, were shown as high-performance metal-free electrocatalysts for the hydrogen evolution.[36] Polypyrrole has also been used as the coating of silicon carbide nanowires to tune their dielectric properties.[37] In order to promote the grafting of polypyrrole onto the surface of silica nanoparticles, the modification with N-(3-trimethoxysilylpropyl)pyrrole was performed.[38] However, so far, silica adducts with pyrrole compounds have not been the main subject of scientific investigations and their behavior as silica coupling agents with unsaturated polymer chains has never been reported.

SP has already been used, by some of the authors, to prepare adducts with sp^2 carbon allotropes,[22,39,40] with high carbon efficiency. Adducts with carbon black were used as reinforcing fillers in elastomeric composites.[40] Hence, the objective of this work was to further explore the potentialities of this *Janus* molecule.

Herein, SP was prepared as already reported.[22,34] The adduct of SP with silica was formed by simply mixing and heating the physical mixture. In the whole process, from the reagents to the adduct, water was supposed to be the only co-product. Characterization of the adduct was carried out by means of solvent extraction, thermogravimetric analysis, attenuated total reflectance−Fourier transform infrared spectroscopy (ATR-IR), and X-ray photoelectron spectroscopy (XPS). The silica/SP adduct was used in elastomeric composites based on poly(styrene-co-butadiene) from solution anionic polymerization (S-SBR) and poly(1,4-*cis*-isoprene) from *Hevea brasiliensis* (Natural rubber, NR) and silica as the only filler. S-SBR and NR are the typical elastomers used in composites for tire treads. Composites with TESPT as the silica coupling agent and without any coupling agent were also prepared. The cross-linking behavior was studied with rheometric tests, the dynamic−mechanical properties were analyzed by applying sinusoidal stresses in the axial mode, and the ultimate properties were assessed by means of tensile tests. To investigate the reactivity between the OH groups of SP and SiOR groups, reactions were performed between SP and diethoxydimethyl silane as model compounds and the products were characterized by means of ^{1}H-NMR and gas chromatography−mass spectrometry (GC−MS). To investigate the reactivity of the pyrrole ring with sulfur-based systems, 1,2,5-trimethylpyrrole (trimethylpyrrole, TMP) was reacted with 1-dodecanthiol (in the presence of azobisisobutyrronitrile (AIBN) and 1-hexyl-2,5-dimethyl-1*H*-pyrrole (hexylpyrrole, HP) was reacted with orthorhombic sulfur, characterizing the products through GC−MS.

2. EXPERIMENTAL SECTION

2.1. Materials and Methods. *2.1.1. Reagents and Solvents.* They were purchased and used without further purification. 2-Amino-1,3-propanediol (Serinol, kindly provided by Bracco), methylamine 40% wt in H_2O (Sigma Aldrich), 1-hexanamine (Sigma Aldrich), ethanolamine (Sigma Aldrich), 2,5-dimethylfuran (Sigma Aldrich), 1-dodecanethiol (Sigma Aldrich), AIBN (2−2′-azaisobutyronitrile, from Sigma Aldrich), carbon tetrachloride (CCl_4) (Sigma Aldrich), and diethoxydimethylsilane (Sigma Aldrich); squalene >98% (Sigma Aldrich); DMSO-d_6 (Sigma Aldrich).

2.1.2. For the Preparation of Rubber Composites. 2.1.2.1. Rubbers. Solution styrene-butadiene rubber (S-SBR) was poly(styrene-co-butadiene) from anionic polymerization promoted by an organo-

https://doi.org/10.1021/acssuschemeng.2c04617
ACS Sustainable Chem. Eng. 2023, 11, 2713−2726

lithium initiator: SPRINTAN SLR-4630 (TRINSEO), with 25% styrene, 37.5 parts of TDAE oil, typical glass transition temperature = −28 °C, Mooney viscosity (ML(1 + 4)100 °C) = 55 MU. The S-SBR is partially Si-coupled and is not functionalized. Natural rubber was poly(1,4-*cis*-isoprene) from *Hevea brasiliensis*: STR20 (Eatern GR Thailand − Chonburi).

2.1.2.2. Silica. Silica ZEOSIL 1165MP (Solvay). The product was in white micropearls. Technical data sheet: specific surface area = 140−180 m^2/g, loss on drying (2 h @ 105 °C) ≤8.0%, soluble salts (as Na_2SO_4) ≤2.0%. For the present work, the silica surface area was determined by using the Brunauer−Emmett−Teller (BET) method. Samples were evacuated at 200 °C for 2 h and N_2 adsorption isotherms were recorded at 77 K in a liquid nitrogen bath, by using a MICROACTIVE TRISTAR II PLUS apparatus. The specific surface area (SSA) was found to be = 160 m^2/g.

The concentration of OH groups on the silica surface, expressed as (the number of OH groups)/(nm^2_{silica}) was estimated by using eq 1.

$$\left[\frac{OH_{Total}}{nm^2}\right] = \frac{\frac{\%\ \text{mass loss of silica}\ (T > 150°C)}{MM_{OH}} \times N_A}{\text{SSA (silica ZEOSIL 1165MP)}} \quad (1)$$

where SSA = 160 m^2/g and N_A (Avogadro's number) = 6.022×10^{23} molecules/mol. The % mass loss of silica was estimated from TGA analysis (see below in the text).

2.1.2.3. Ingredients. 4,4,15,15-Tetraethoxy-3,16-8,9,10,11-tetrathia-4,15-disilaoctadecane (TESPT) (Evonik), stearic acid (Sogis), ZnO (Zincol Ossidi), *N*′-phenyl-*p*-phenylenediamine (6PPD) (Crompton), sulfur (Solfotecnica), and *N*-ter-butyl-2-benzothiazyl sulfenamide (TBBS) (Flexyis).

2.2. Synthesis and Characterization of Pyrrole Derivatives (PyC). *2.2.1. Synthesis of 2-(2,5-dimethyl-1H-pyrrol-1-yl)propane-1,3-diol (SP).* In a 250 mL round-bottom flask equipped with a magnetic stirrer, a mixture of 2,5-hexanedione (41.4 g; 0.36 mol) and serinol (30.0 g; 0.36 mol) was introduced. The reagents were in a stoichiometric amount. The mixture was then stirred at 150 °C for 3 h. After this time, the reaction mixture was cooled to room temperature. Pure products (55 g) were obtained, with 96% yield. The yield was calculated by using the following expression: 100 × (weighed mass of SP)/(theoretical mas of SP).

^{1}H NMR ($CDCl_3$, 400 MHz); δ (ppm) = 2.27 (s, 6H); 3.99 (m, 4H); 4.42 (quintet, 1H); 5.79 (s, 2H). ^{13}C NMR (DMSO-d_6,100 MHz); δ (ppm) = 127.7; 105.9; 71.6; 61.2; 13.9.

2.2.2. Synthesis of 1,2,5-Trimethylpyrrole (TMP). In a 100 mL round-bottom flask equipped with a magnetic stirrer and condenser was added methylamine 40%wt in H_2O (0.097 mol, 8.36 mL).

At 0 °C, 2,5-hexanedione (HD, 0.097 mol, 11.37 mL) was added dropwise; after HD addition, the flask was placed in an oil bath and the reaction temperature was set at 130 °C for 4 h. At the end of the reaction, two phases were observed: an oil phase (corresponding to the product) and a water phase. The product was pipetted out and collected in a 100 mL round-bottom flask. A dark brown liquid (6.76 g) was obtained, which was weighed, with 64% yield, and calculated as reported above.

^{1}H NMR ($CDCl_3$, 400 MHz); δ (ppm) = 5.78 (s, 2H), 3.38 (s, 3H), 2.21 (s, 6H).

2.2.3. Synthesis of 1-Hexyl-2,5-dimethyl-1H-pyrrole (Hexylpyrrole, HP). 1-Hexanamine (9.88 mmol, 1 g) was fed into a 100 mL round-bottom flask equipped with a magnetic stirrer and a condenser. The temperature was set at 130 °C. 2,5-Hexanedione (HD, 9.88 mmol, 1.16 mL) was then added dropwise. The reaction was left to stir at 130 °C for 3 h. After this time, the reaction mixture was cooled to room temperature and water was removed at reduced pressure.

Dark brown liquid (1.50 g) corresponding to HP was obtained, with 85% yield, and calculated as reported above. HP was characterized by means of ^{1}H NMR.

^{1}H NMR ($CDCl_3$, 400 MHz) δ (ppm) δ 5.81 (s, 2H), 3.85−3.70 (m, 2H), 2.28 (s, 6H), 1.76−1.61 (m, 2H), 1.45−1.31 (m, 6H), 1.03−0.91 (m, 3H). ^{13}C NMR ($CDCl_3$, 100 MHz) δ (ppm) 128.98, 128.03, 106.37, 106.00, 56.60, 49.56, 48.26, 44.712, 41.82, 39.91, 35.26, 32.68, 27.62, 23.68, 14.22.

2.2.4. Synthesis of 2-(2,5-Dimethyl-1H-pyrrol-1-yl)ethan-1-ol (Ethanol Pyrrole, EP). Ethanolamine (0.071 mol, 4.33 g) was fed into a 100 mL round-bottom flask equipped with a magnetic stirrer and a condenser. The temperature was then set at 155 °C and 2,5-hexanedione (HD, 0.071 mol, 8.35 mL) was added dropwise. After 3 h, the reaction was stopped by cooling to room temperature. A brown solid (10 g) corresponding to the product 2-(2,5-dimethyl-1*H*-pyrrol-1-yl)ethan-1-ol (ethanol pyrrole, EP) was obtained with 90% yield, calculated as reported above. EP was characterized by means of ^{1}H and ^{13}C NMR.

^{1}H NMR ($CDCl_3$, 400 MHz) δ (ppm) 5.79 (s, 2H), 3.90 (dt, 2H), 3.75 (dd, 2H), 2.23 (s, 6H).

^{13}C NMR ($CDCl_3$, 100 MHz) δ (ppm) 126.08, 103.68, 75.40, 75.09, 74.77, 60.34, 43.62, 10.71.

2.3. Preparation of Physical Mixtures and Adducts between Silica and SP. *2.3.1. Preparation of a Physical Mixture between Silica and SP. 2.3.1.1. Physical Mixture Silica: SP = 10:1.* In a 100 mL round-bottom flask equipped with a magnetic stirrer were poured in sequence 10 g of silica and 25 mL of acetone. One gram of the pyrrole compound (for preparing a 10/1 by mass physical mixture), diluted with some milliliters of acetone, was added into the system under magnetic stirring (300 rpm). The system was then left under stirring at room temperature for 10 min. The solvent was then completely removed under reduced pressure.

2.3.2. Preparation of the Adduct between Silica and SP. 2.3.2.1. Adduct Silica: SP = 10:1. In a 250 mL round-bottom flask equipped with a magnetic stirrer were poured in sequence 10 g of silica and 1 g of the pyrrole compound, diluted with some milliliters of acetone, which were added dropwise under magnetic stirring (300 rpm). The flask was then put into an oil bath set at 60 °C, under magnetic stirring until complete evaporation of the solvent. The dried powder was left at 150 °C for 2 h under magnetic stirring (300 rpm), which was then brought to room temperature and was finally thoroughly washed with acetone in a Soxhlet extractor for 16 h. The powder was finally dried in an oven at 80 °C for 6 h. The functionalization yield, calculated as explained below in the text, was found to be 96%.

2.3.2.2. Adduct Silica: SP = 10:0.45. The same procedure reported above for the 10:1 adduct was followed, except that 450 mg of SP was used instead of 1 g. The functionalization yield, calculated as explained below in the text, was found to be 87%.

2.3.3. Functionalization Yield. The functionalization yield was calculated by applying eq 2, by using data from TGA analysis.

$$\text{Functionalization yield (\%)} = 100 \times \frac{\text{SP mass\%in (silica − SP adduct) after acetone washing}}{\text{SP mass\%in (silica − SP adduct)theoretical}} \quad (2)$$

2.3.4. Preparation of SP on Silica and Preparation of Silica/SP Adducts. Silica Zeosil 1165 MP (16 g) was put in a 500 mL round-bottom flask, together with 30 mL of deionized water. Then, two water solutions were added: one made using 0.86 g of serinol (9.4 mmol) in 10 mL of water and the other made using 1.08 g of 2,5-hexanedione (9.4 mmol) in 10 mL of water. The mixture was stirred in an open flask at 105 °C (350 rpm) until the full evaporation of the solvent (around 2 h), then the temperature was increased at 150 °C and the reaction was carried out for 2 h. The product was placed in a cellulose thimble and put in a Soxhlet extractor with acetone for 12−16 h, then recovered as an orange powder. The functionalization yield, calculated by using eq 2, was found to be 95%, and only a minor amount of SP was extracted.

2.4. Preparation of Elastomer Composites. Elastomer composites were prepared via melt blending by using a 55 cc Brabender internal mixer, and formulations are given in Table 1. The quantities of the ingredients are expressed in phr = parts per hundred rubber.

The same amount of sulfur atoms was used in all the composites. Taking into account that the atomic weight of sulfur is 32.06 Da and

https://doi.org/10.1021/acssuschemeng.2c04617
ACS Sustainable Chem. Eng. 2023, 11, 2713−2726

Table 1. Formulations of Silica-Based Composites with Different Coupling Agents for Silica[a]

	silica (phr)	silica/TESPT (phr)	silica/SP (phr)
S-SBR[b]	110	110	110
NR[c]	20	20	20
silica	50	50	0
TESPT	0	4	0
silica/SP[d]	0	0	54.5
sulfur	2.9	2.0	2.9

[a]Other ingredients: ZnO 2.5, stearic acid 2, 6PPD 2.0, sulfur 2.9, TBBS 1.8. [b]SPRINTAN SLR-4630, see the experimental part for the technical data. [c]STR20, see the experimental part for the technical data. [d]Silica: 50 phr, SP 4.8 phr.

the molecular weight of TESPT is 534.50 Da, it was calculated that the mass % of sulfur in TESPT is 23.97 and that the phr of sulfur in TESPT are 0.95. Hence, 2.9 phr of sulfur were used in the composite with silica/SP adducts.

2.4.1. Experimental Procedure. S-SBR (29.8 g) and 5.4 g of NR were introduced into the Brabender at a temperature of 140 °C for 2 min at 60 rpm. Then, 13.4 g of silica ZEOSIL 1165MP (pristine or modified with PyC) with 1.0 g of TESPT, if present, and stearic acid were added into the mixer and mixed at the same temperature for 4 min at 60 rpm. The composite was then discharged and cooled at room temperature. The masterbatch was then introduced into the Brabender at a temperature of 50 °C for 2 min at 60 rpm. After that, 0.53 g of 6PPD and 0.67 g of zinc oxide were added and mixed at the same temperature for 2.5 min at 60 rpm. Then, 0.48 g of TBBS and sulfur were finally added and mixed for 2.5 min at 60 rpm. This procedure was adopted in previous studies, for example, ref 41: sulfur and sulfenamide are added after ZnO and 6PPD, in the same mixing step, without discharging the composite. The final rubber composite was discharged and cooled at room temperature and by finally passing five times on a two-roll mill operating at room temperature.

2.5. Studies To Elaborate the Mechanism for the Reaction of SP with Silica, the Sulfur-Based Cross-Linking System, and the Unsaturated Elastomer. *2.5.1. Reaction of 2-(2,5-Dimethyl-1H-pyrrol-1-yl)propane-1,3-diol (SP) with Diethoxydimethylsilane.* SP (0.5 g) (2.96 mmol) was put in a 100 mL round-bottom flask equipped with a magnetic stirrer and a condenser. The temperature was set at 150 °C, and 0.51 mL of diethoxydimethylsilane (2.96 mmol) was added dropwise. The reaction was monitored by means of GC−MS and was stopped after 12 h by cooling to room temperature.

2.5.2. Reaction of 2-(2,5-Dimethyl-1H-pyrrol-1-yl)ethan-1-ol (EP) with Alcoxysilanes. EP (0.42 g) (3.03 mmol) was fed into a 100 mL round-bottom flask equipped with a magnetic stirrer and a condenser. The temperature was then set at 150 °C, and 0.35 mL of diethoxydimethylsilane (2.02 mmol) was added dropwise. The reaction was monitored by means of ^{1}H NMR and was stopped, after 12 h, by cooling to room temperature.

2.5.3. Reaction of 1,2,5-Trimethylpyrrole (TMP) with Dodecanthiol (DSH). In a 100 mL round-bottom two-neck flask equipped with a magnetic stirrer and a condenser, TMP (2.75 mmol, 0.3 g) and DSH (2.75 mmol, 0.56 g) were fed in CCl_4 as a solvent and under a N_2 atmosphere, at 95 °C. After 1 h, the radical initiator (AIBN, 3% mol with respect TMP) was added. The reaction mixture was left to stir until the disappearance of TMP which was checked by means of TLC (Hexane/EtOAc 9.5:0.5). Multiple additions of AIBN were necessary to reach a reasonable conversion of TMP. After 12 h, the reaction was stopped just by removing the reagents under reduced pressure.

2.5.4. Reaction of 1-Hexyl-2,5-dimethyl-1H-pyrrole (HP) with Sulfur. In a 10 mL two-neck round-bottom flask equipped with a magnetic stirrer and a nitrogen balloon, S_8 was added (0.53 mmol, 0.136 g). The flask was placed in an oil bath at 170 °C. After complete melting of sulfur, HP (0.53 mmol, 0.1 g) was added dropwise. The reaction was left stirring for 6 h and monitored by means of GC−MS.

2.5.5. Reaction of Trimethylpyrrole with Sulfur. In a 10 mL two-neck round-bottom flask equipped with a magnetic stirrer and a nitrogen balloon, S_8 was added (0.53 mmol, 0.136 g). The flask was placed in an oil bath at 170 °C. After complete melting of sulfur, the temperature was taken to 158 °C and TMP (0.53 mmol, 0.057 g) was added dropwise. The reaction was left stirring for 6 h and monitored by means of GC−MS.

2.5.6. Reaction of Sulfurated Trimethylpyrrole with Squalene. In a 10 mL two-neck round-bottom flask equipped with a magnetic stirrer and a nitrogen balloon, sulfurated trimethyl pyrrole (0.53 mmol, 0.109 g) and squalene (0.53 mmol, 0.216 g) were added in sequence. The flask was placed in an oil bath at 170 °C. The reaction was left stirring for 30 min and monitored by means of ^{13}C NMR spectroscopy.

^{13}C NMR (DMSO-d_6, 100 MHz) δ (ppm): 134.3; 134.1; 133.6; 133.5; 130.5; 128; 126.6; 126.2; 123.9; 123.8; 123.7; 110.3; 108.3; 30.5; 29.5; 27.6; 26; 25; 17.4; 15.6; 12; 11.9; 11.8; 10.5; 10.2.

2.6. Characterization Techniques. *2.6.1. Thermogravimetric Analysis.* Thermogravimetric analysis (TGA) tests under N_2 flow (60 mL/min) were performed using a Mettler TGA SDTA/851 instrument according to the standard method ISO9924-1. Samples (10 mg) were heated from 30 to 300 °C at 10 °C/min, kept at 300 °C for 10 min, and then heated up to 550 °C at 20 °C/min. After being maintained at 550 °C for 15 min, they were further heated up to 900 °C with a heating rate of 30 °C/min and kept at 900 °C for 20 min under flowing air (60 mL/min).

2.6.2. Attenuated Total Reflectance Infrared (ATR-IR). The analyses were carried out with a Perkin Elmer Spectrum 100: 1 cm^{-1} resolution, range of 650−4000 cm^{-1}, 16 scans.

2.6.3. Nuclear Magnetic Resonance. ^{1}H-NMR and ^{13}C-NMR spectra were recorded on a Bruker 400 MHz (100 MHz ^{13}C) instrument at 298 K. Chemical shifts were reported in ppm with the solvent residual peak as the internal standard (DMSO-d_6: δ_H = 2.50 ppm, $CDCl_3$: δ_H = 7.26 ppm).

2.6.4. High-Resolution X-ray Photoelectron Spectroscopy. Survey scan and high-resolution XPS spectra were collected by means of a PHI 5000 VersaProbe instrument (Physical Electronics). Analyses were performed in UHV conditions (10^{-8} Pa) with a monochromatic Al K-alpha X-ray source (energy: 1486.6 eV; voltage: 15 kV voltage; anode current: 1 mA) and a power of 25.2 W. Survey and high-resolution spectra were acquired using a pass energy of 187.85 and 23.5 eV, respectively. A take-off angle of 45°, a 100 μm diameter X-ray spot size, and a double beam (electron and argon ion gun) neutralization system, dedicated to reduce the charging effect on samples, were employed. The samples were placed in the XPS pre-chamber overnight, in order to avoid anomalous outgassing during data acquisition. Spectra were analyzed by Multipak 9.6 software, and the core-level binding energies of all spectra were referenced to the C 1s line at 284.5 eV. Peak deconvolution of high-resolution Si 2p, O 1s, and C 1s spectra was performed by PeakFit software.

2.6.5. Characterization of Elastomer Composites. 2.6.5.1. Cross-Linking. It was carried out in a rubber process analyzer (RPA, Alpha Technologies, Hudson, OH, USA). Crude rubber composites (5 g) were placed in the rheometer. As done in previous studies, for example, in ref 42, a first strain sweep (0.1−25% strain amplitude) was performed at 50 °C on noncross-linked samples, to cancel the thermo-mechanical history of the rubber composite. Then, the sample was kept at 50 °C for 10 min and subjected to another strain sweep at 50 °C. Cross-linking was then performed at 170 °C, with an oscillation angle of 6.28° at a frequency of 1.7 Hz. The torque versus time was measured, determining the minimum torque(M_L), the maximum torque (M_H), the time needed to have a torque equal to M_L + 1 dN m (t_{S1}), and the time needed to reach 90% of the maximum torque (t_{90}).

2.6.6. Cross-Link Density. Equilibrium swelling measurements were carried out at 20 °C, in toluene. Specimens (1 mm × 15 mm × 15 mm) were used for the measurement.

2.6.6.1. Total Cross-Link Density. Reagents were allowed to diffuse in the specimens kept in n-heptane, for two days, under nitrogen. n-Heptane was drained, the specimens were washed with petroleum

https://doi.org/10.1021/acssuschemeng.2c04617
ACS Sustainable Chem. Eng. 2023, 11, 2713−2726

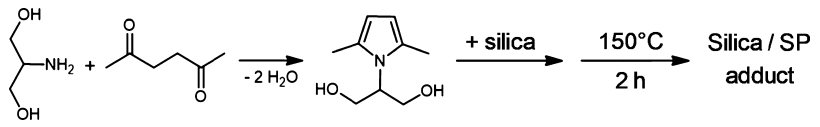

Figure 2. Preparation of the silica/serinol pyrrole adduct.

ether, and they were dried overnight at room temperature under reduced pressure. Specimens were then immersed in 200 mL of toluene in a glass tube flashed with nitrogen and closed with a stopper, and they were left in the dark for 72 h, time commonly considered suitable to reach the equilibrium swelling state. Samples were then taken from the glass tube, and the excess solvent was removed by blotting the samples with a filter paper. Samples were finally and rapidly placed in a clean closed small container and were weighed. Samples were then dried for 24 h under vacuum at 70 °C, to remove the solvent, and were then weighed again, to obtain the weight of the dry network and the amount of the sorbed solvent.

Flory–Rehner equation, eq 3, was then used to calculate the cross-link density:

$$\nu_e = \frac{-[\ln(1 - V_r) + V_r + X_1 \times V_r^2}{\left[\frac{V_1(V_r^{1/3} - V_r)}{2}\right]} \quad (3)$$

where ν_e = effective number of chains in a real network per unit volume, V_r = volume fraction of polymer in a swollen network in equilibrium with pure solvent and is calculated with eq 4:

$$V_r = \frac{\text{weight of dry rubber/density of dry rubber}}{\frac{\text{weight of dry rubber}}{\text{density of dry rubber}} + \frac{\text{weight of solvent absorbed by sample}}{\text{density of solvent}}} \quad (4)$$

χ_1 = polymer–solvent interaction parameter (0.391 at 25 °C for cis polyisoprene as the polymer and toluene as the solvent). V_1 = molecular volume of the solvent.

2.6.6.2. Mono- and Di-Sulfidic Cross-Links Measurement. For this measurement, the following procedure was adopted. In a 200 mL beaker, 100 mg of the cross-linked composite and 100 mL of heptane were placed, in sequence. The sample was left in heptane for 24 h without stirring and were then added 4 mL of piperidine and 3.8 mL of 1-propanethiol, leaving this mixture at room temperature for 2 h. The mixture was first washed with heptane (3 times with 50 mL) and then filtered. The solid was left again in heptane (50 mL). After 24 h, the solvent was removed, the solid was washed with petroleum ether (3 times with 50 mL), and then filtered using a vacuum pump. The solid obtained was left in 50 mL of petroleum ether for 2 h, then was filtered under vacuum. Further drying was performed under vacuum for 24 h. The resulting sample was again immersed in 200 mL of toluene for 72 h to achieve the equilibrium swelling state. The same procedure reported above for the measurement of the total cross-link density was followed.

This method was chosen under the assumption that the silica/SP adduct has no interactions with 1-propanethiol or piperidine. As to the interaction with 1-propanethiol, it is shown below in the text that only the mono-addition of thiol to the pyrrole ring was documented and that only hexylpyrole derivatives with only one sulfur ring were detected. Hence, it can be assumed that, after the reaction with sulfur and sulfur-based chemicals, which occurs in vulcanization, the pyrrole ring does not give rise to interactions with propanethiol. As to the interaction with piperidine, an acid–base interaction was not expected, as the pyrrole on the silica/SP adduct lacks centers at a pK_a value which could allow the occurrence of the acid–base reaction with piperidine.

2.6.7. Dynamic–Mechanical Characterization in the Axial Mode. Dynamic–mechanical properties were measured using an Instron dynamic device in the traction–compression mode according to the following methods. A test piece of the cross-linked elastomeric composition, having a cylindrical form (length = 25 mm; diameter = 12 mm) and kept at the prefixed temperature (10, 23 and 70 °C) for the whole duration of the test, was compression-preloaded up to 25% longitudinal deformation with respect to the initial length and then submitted to a dynamic sinusoidal strain having an amplitude of ±3.5% with respect to the length under pre-load, with a 100 Hz frequency. The dynamic–mechanical properties are expressed in terms of dynamic storage modulus (E') and loss factor (tan Delta) values. The tan Delta value is calculated as a ratio between loss (E'') and storage modulus (E').

2.6.8. Tensile Test. Tensile measurements were performed on samples of the elastomeric composites vulcanized at 175 °C for 20 min. Stresses at 50, 100, and 300% elongation (respectively σ_{50}, σ_{100}, and σ_{300}), stress at break (σ_B), elongation at break (ε_B), and the energy required to break were measured according to Standard ISO 37:2005.

3. RESULTS AND DISCUSSION

3.1. Preparation of Silica/SP Adducts. SP was synthesized and characterized as already reported,[22,34] by mixing serinol and 2,5-hexandione, heating then the mixture at 150 °C for 3 h. The yield of the reaction, in line with the previous reports, was about 96% and the atom efficiency was thus about 83%. The adduct of SP with silica was prepared as described in detail in the experimental part, by using 10 parts of SP/100 parts of silica (9.1% mass of SP). In brief: SP was distributed on silica with the help of acetone. Sampling of the physical mixture was carried out and the TGA results revealed the homogeneity of the SP distribution on silica: the variation coefficient of the SP content was lower than 2%. The mixture was then heated at 150 °C for 2 h. The whole process for the preparation of the silica/serinol pyrrole adduct, summarized in Figure 2, is characterized by water as the only co-product. The carbon economy,[18,21] which is the percentage of carbon in the useful product (the adduct) with respect to the total carbon in the reactants, is 100%.

The adduct was then thoroughly extracted with acetone.

It could be reasonably argued that the preparation of the silica/SP adduct by solvent mixing is complicated and that the use of solvents is not environment-friendly. However, such a procedure was adopted in the laboratory scale, with the objective to promote the homogenous dispersion of SP and silica. For the scale up of the reaction, the use of a spray drier[43] could reasonably be hypothesized. Moreover, SP could be also prepared in situ on silica, by mixing serinol and 2,5-HD, heating then the mixture. This procedure was adopted for the preparation of the silica/SP adduct. Details are in the experimental part. In brief, water solutions of serinol and 2,5-hexanedione (the two reagents were in equimolar ratio) were poured inside a reaction flask together with silica. The amounts of serinol and HD were calculated in order to obtain 1:10 as the mass ratio between serinol pyrrole and silica. After water evaporation, the reaction for the adduct preparation was carried out at 150 °C for 2 h. The IR spectrum of the adduct, taken after acetone extraction, reported in the Supporting Information in Figure S.2 and discussed below in the text, revealed the presence of the typical spectral features of the pyrrole compound in the adduct.

3.2. Characterization of Silica/SP Adducts. *3.2.1. Thermogravimetric Analysis.* TGA was performed on pristine

https://doi.org/10.1021/acssuschemeng.2c04617
ACS Sustainable Chem. Eng. 2023, 11, 2713−2726

silica and on silica/SP adducts, before and after acetone extraction. Data are in Table 2 for the adduct silica: SP = 10:1.

Table 2. Mass Loss (Mass %) for Pristine Silica and Silica/SP Adducts from TGA, before and after Acetone Extraction

	mass loss 30 °C < T < 150 °C	mass loss 150 °C < T < 900 °C
silica	5.0	3.0
silica/SP before extraction	4.1	12.8
silica/SP after extraction	3.7	12.5

Interpretation of the TGA results was made on the basis of what is reported in the literature.[44−50] In all the samples, the mass loss between 30 and 150 °C was attributed to the water adsorbed onto the surface of silica. The silica/SP adduct revealed a lower mass loss with respect to the pristine silica. This could be ascribed to the increased hydrophobicity of the adduct as well as to the water released during its preparation. The mass loss of pristine silica in the range from 150 to 900 °C was attributed to the silanols. In the literature,[50] this value of mass loss was used to estimate the amount of OH groups on the silica surface, typically expressed as the number of OH groups/nm^2, by using eq 1 (see the experimental part). In the case of the silica sample used in this work, by considering 160 m^2/g as the value of surface area experimentally determined, a value of 6.64 $OH_{molecules}/nm^2$, which corresponds to 176 $mmol_{(OH)}/100\ g_{(silica)}$, was calculated. It was also reported[51] that the isolated silanols are the most reactive sites on the silica surface and they were estimated[51] to be 25% of the total amount of silanols. In the silica sample used for this work, the number of isolated silanols was thus equal to 44.2 $mmol_{(OH)}/100\ g_{(silica)}$. Hence, the stoichiometric amount of SP, for the reaction with isolated silanols, would be 7.5 g/100 g of silica. In this work, an excess of SP (10 g SP/100 g of adduct), with respect to the isolated silanols, was used. The amount of SP in the adduct was estimated on the basis of the mass loss in the range from 150 to 900 °C, subtracting the mass loss of pristine silica in the same temperature range. The amount of SP in the silica/SP adduct was 9.8 and 9.5%, for the adduct before and after acetone extraction, respectively. The TGA analysis, which appears to overestimate the amount of SP in the adduct, reveals, however, a high functionalization yield, i.e., 96%, calculated by using eq 2.

3.2.2. Elemental Analysis. Elemental analysis was performed on the silica/SP adduct, after acetone extraction. The experimental values of C% and N% were compared with the theoretical values calculated on the basis of the initial amount of SP in the adduct (9.1% mass). As shown in Table S.1 in the Supporting Information, very similar values were obtained.

TGA and elemental analysis results allow us to conclude that the functionalization reaction was characterized by a quantitative yield and that an SP amount larger than the stoichiometric one with respect to the isolated silanols remained on the silica surface.

3.2.3. Infrared Spectroscopy. ATR-IR spectra were collected in the wavelength range between 700 and 4000 cm^{-1}. As shown in Figure 3, the spectra of silica (a), silica/SP adduct (b), silica/SP adduct upon subtracting the spectrum of silica (c) and pristine SP (d) are reported.

The spectrum of silica (Figure 3a) can be interpreted on the basis of what is reported in the literature.[49,50] The absorption bands arising from the asymmetric vibration of SiO could be detected around 1100 cm^{-1}.[52,53] Asymmetric vibrations of SiOH and symmetric vibrations of SiO are visible at 795 and 950 cm^{-1}, respectively. The absorption bands between 800 and 1260 cm^{-1} have been described as the superimposition of various SiO_2 peaks, SiOH bonding, and peaks due to residual organic groups. Water shows an intense characteristic absorption band between 3300 and 3500 cm^{-1}, due to OH stretching in H-bonded water. Also, this band can be cross-checked through the 1635 cm^{-1} band due to the scissor bending vibration of molecular water.

In the spectrum of SP (Figure 3d), the broad band from 3370 to 3330 cm^{-1} is reasonably due to the hydrogen-bonded OH groups, the peaks from about 1550 to 1000 cm^{-1} can be attributed to the vibrations of the pyrrole ring, and the peak at 760 cm^{-1} is due to the C−H out-of-plane bending.

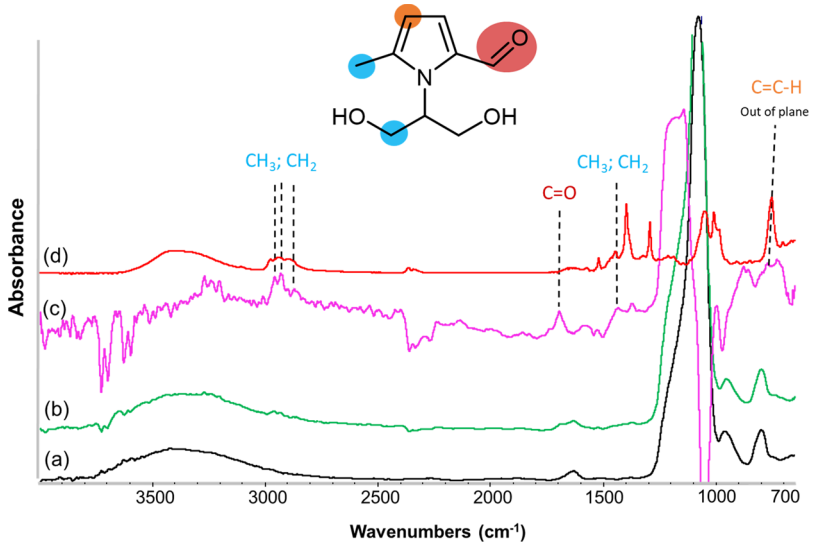

Figure 3. FT-IR spectra of pristine silica (a, black curve), adduct silica/SP (b, green curve), adduct silica/SP upon subtracting the spectrum of silica (c, purple curve), and SP (d, red curve).

https://doi.org/10.1021/acssuschemeng.2c04617
ACS Sustainable Chem. Eng. 2023, 11, 2713−2726

Table 3. Chemical Composition from the XPS Analysis of Pristine Silica and Silica/SP, Physical Mixture, and Adducts Prepared at Different Temperatures

sample	silica−SP ratio	reaction temperature (°C)	chemical compositions C	O	Si	N	N/Si
silica			13.2	62.8	22.9		
physical mixture	10:1		25.0	51.4	21.4	2.2	0.1
adduct silica/SP	10:1	room temperature	3.6	64.1	27.0	0	0
adduct silica/SP	10:1	80	11.6	61.6	25.4	0.9	0.04
adduct silica/SP	10:1	150	21.3	53.7	22.6	2.1	0.09
adduct silica/SP	10:1	180	24.3	51.4	21.7	2.1	0.10

The spectra of the silica/SP adducts are shown in Figure 3b,c. Upon subtracting the spectrum of silica (Figure 3c), it is possible to identify the peaks typical of the pyrrole compound. The assignments are supported by the analysis of the IR spectra of silica/SP physical mixtures (from 1:0.3 to 1:1 as the mass ratio), which are shown in Figure S.1 in the Supporting Information. These findings suggest that the reaction for the formation of the adduct does not appreciably alter the chemical structure of the pyrrole compound. Figure S.2 reports the IR spectrum of the silica/SP adduct obtained by performing the synthesis of SP on silica, by mixing serinol and 2,5-HD, and then heating the mixture at 150 °C for 2 h. Also, in this case, upon subtracting the spectrum of silica, it is possible to identify the peaks typical of the pyrrole compound. Peaks which can be attributed to $-CH_2$ and $-CH_3$ and to the carbonyl due to the oxidation of the methyl group are clearly visible.

3.2.4. XPS Analysis. Silica/SP adducts (10:1 as mass ratio) were prepared by using different reaction temperatures (room temperature, 80, 150, and 180 °C) and were thoroughly washed with acetone. The washed adducts and the silica/SP physical mixture (10:1 mass ratio, not washed) were analyzed by XPS.

3.2.5. Chemical Composition of the Samples. The chemical compositions of the adducts, obtained from XPS analysis, are shown in Table 3.

The surface of pristine silica had a Si/O ratio (0.4) close to the expected one. Moreover, some carbon contaminations were found, in line with what is reported in the literature.[54] As expected, nitrogen was detected in the physical mixture and in the silica/SP adduct samples, but it was absent in the spectrum of pristine silica. Hence, its signal was taken as the marker for the presence of the pyrrole compound onto the surface of silica. The intensity of the peaks of Si 2p and O 1s decreased, while that of the peaks of C 1s and N 1s increased with reaction temperature, due to higher coverage of the surface by SP molecules. The N/Si ratio for the physical mixture (not washed) was equal to 0.10. The same ratio was found for the adducts treated at 150 and 180 °C for 2 h. Moreover, no significant differences as to the C 1s, O 1s, Si 2p, and N 1s content were noticed between the silica/SP adducts prepared at 150 °C and at 180 °C. Nitrogen was not found in the adduct treated at room temperature, while the N/Si ratio was 0.04 for the adduct treated at 80 °C. It is thus clear that upon increasing the reaction temperature, the surface concentration of SP molecules in the adduct increases. These findings suggest that the adduct is not formed or is formed in a minor amount when the thermal treatment is performed at temperatures up to 80 °C.

3.2.6. High-Resolution Spectra. The high-resolution XPS Si 2p, O 1s, and C 1s spectra were analyzed and deconvoluted to access the chemical bonds of the samples involving such elements. The high-resolution Si 2p spectra were fitted with three components, assigned as follows:[55] Si1 at 104.2 eV attributed to Si−O−H groups of silica; (ii) Si2 at 103.4 eV attributed to Si−O−Si groups;

(iii) Si3 at 102.6 eV attributed to Si−O−C groups formed during the reaction between silica and SP. Data derived from the spectra are collected in Table 4.

Table 4. Data from High-Resolution Si 2p Spectra of Pristine Silica and Silica/SP Physical Mixture and Adducts Prepared at Different Temperatures

sample	silica/SP ratio	reaction temperature (°C)	Si1	Si2	Si3
silica			51.3	48.7	0
physical mixture	10:1		13.9	50.5	35.6
adduct silica/SP	10:1	room temperature	52.1	38.7	9.1
adduct silica/SP	10:1	80	7.1	44.1	48.8
adduct silica/SP	10:1	150	1.8	38.7	59.5
adduct silica/SP	10:1	180	1.6	42.7	55.6

For the silica/SP adducts, the signal attributed to Si−O−H (Si1) decreased, whereas the signal attributed to Si−O−C (Si3) increased by increasing the reaction temperature. A substantial difference was observed bringing the temperature from room temperature to 80 °C and a minor difference was observed when the temperature was brought to 150 °C. Values for the samples obtained at 150 and 180 °C are very similar. In the physical mixture, more SP products (higher Si3 component) than those in the corresponding adduct obtained at room temperature were detected, probably due to the fact that the former is not washed. However, the higher Si3 component for the adducts obtained at 80−180 °C, in comparison with the physical mixture, confirms the reaction occurrence.

The high-resolution XPS O 1s spectra were deconvoluted and the obtained peaks were assigned as follows:[55] (i) O1 at 534.1 eV attributed to −O−H groups of silica and SP; (ii) O2 at 532.4 eV attributed to −O−Si and −O−C groups; (iii) O3 at 530.2 eV attributed to O═C groups. Data derived from the analyzed spectra are in Table 5.

The O1 signal could arise from both the Si−O−H group of silica and from the C−O−H group of SP. Analogously, the O2 signal could arise from the Si−O−Si group of silica, the C−O group of SP, and the Si−O−C group of the adduct. By increasing the reaction temperature (from room temperature

https://doi.org/10.1021/acssuschemeng.2c04617
ACS Sustainable Chem. Eng. 2023, 11, 2713−2726

Table 5. Data from High-Resolution O 1s Spectra of Pristine Silica and Silica/SP Physical Mixture and Adducts Prepared at Different Temperatures

sample	silica−SP ratio	reaction temperature (°C)	O1	O2	O3
silica			11.7	88.3	0
physical mixture	10:1		3.3	95.1	1.6
adduct silica/SP	10:1	room temperature	41.6	55.5	2.9
adduct silica/SP	10:1	80	6.6	92.1	1.3
adduct silica/SP	10:1	150	2.7	95.0	2.3
adduct silica/SP	10:1	180	3.2	94.8	2.0

to 180 °C), the −O−H groups (O1) decrease and the −O−Si and −O−C groups (O2) increase. As reported above for the Si 2p signals, relevant difference is observed from room temperature to 80 °C and a minor difference from 80 to 150 °C, whereas the values for the samples prepared at 150 and 180 °C are comparable. Thus, also at 80 °C, the reaction seems to occur to a good extent. Moreover, as above, data show a higher quantity of SP product on the surface of the physical mixture compared to the corresponding adduct obtained at room temperature. The adducts formed at high temperatures seem to have a higher coverage of the surface by SP molecules, in comparison with the physical mixture.

The high-resolution XPS C 1s spectra were fitted with three components, assigned as follows:[55,56] (i) C1 at 287.9 eV attributed to C−O−Si and C═O groups formed during the reaction; (ii) C2 at 285.5 eV attributed to C−O and C−N groups of SP; (iii) C3 at 284.3 eV attributed to sp^2 carbon atoms, C−C, and C−H groups of SP. Data derived from the analyzed spectra are shown in Table 6.

Table 6. Data from High-Resolution C 1s Spectra of the Physical Mixture and Adduct Silica/SP

sample	silica−SP ratio	reaction temperature (°C)	C1	C2	C3
physical mixture	10:1		6.9	62.7	30.4
adduct silica/SP	10:1	180	13.0	69.7	17.3

The presence of the C1 signal can be explained with the oxidation of the methyl group of the pyrrole ring, which occurs during the preparation of the adduct.

The findings from XPS analysis thus indicate that the reaction occurred between the silanol groups and SP, which can reasonably be assumed to lead to the formation of covalent bonds and which comes to completeness at 150 °C after 2 h.

3.3. Preparation and Characterization of Elastomeric Composites. An elastomeric composite, based on NR and S-SBR, was prepared with the silica/SP adduct described in the previous paragraph. Reference composites were also prepared, with TESPT as the silica coupling agent and without any coupling agent. TESPT was used in the traditional amount, 8% by mass with respect to silica. The amount of sulfur atoms, taking into account both the orthorhombic sulfur and the sulfur bound in TESPT, was the same in all the composites. The formulations of the composites are shown in Table 1 in the Experimental part, where it is also described the procedure for their preparation. In brief, in the first phase, the filler (with or without the coupling agent) and stearic acid were added into the rubber matrix at 140 °C. This temperature was selected to promote the reaction between silica and TESPT. Then, in the second phase, the activator (ZnO), sulfur, and the accelerator were added at 50 °C. The composite was finally homogenized on the two-roll mill.

3.3.1. Sulfur-Based Cross-Linking. All the samples were cross-linked at 170 °C for 20 min. The values of the minimum modulus M_L, the maximum modulus M_H, the induction time t_{S1}, the optimum vulcanization time t_{90}, and the cross-linking rate $(M_H - M_L)/(t_{90} - t_{S1})$ are shown in Table 7. The graphs reporting the modulus versus the cross-linking time are shown in Figure S.3 in the Supporting Information.

Table 7. M_L, M_H, t_{S1},t_{90} Values, and the Vulcanization Rate for the Composites of Table 1

	silica	silica/TESPT	silica/SP
M_L	6.4	2.8	3.6
M_H	25.2	14.9	16.2
t_{S1}	1.9	3.3	1.9
t_{90}	11.0	11.8	11.0
$(M_H - M_L)/(t_{90} - t_{S1})$	2.1	1.4	1.4

The composite with silica without any coupling agent revealed much higher values of M_L and M_H, as expected. Indeed, M_L is an index of the composite viscosity and silica is not shielded, in the absence of a coupling agent. Also, the highest value of M_H can be ascribed to the strong filler-filler network, in the absence of the coupling agent. In fact, the extent of the strain amplitude explored during the cross-linking experiment is not enough for the complete disruption of the filler network. The lowest value of M_L was obtained with TESPT, whereas SP led to a slightly higher M_L value, thus revealing a moderately lower ability to shield silica. The higher M_H value obtained with silica/SP, with respect to silica/TESPT, could be not only due to the lower shielding ability of SP but also to a different structure of the cross-linking network, as discussed below in the text.

The lowest values of the induction time of vulcanization (t_{S1}) could be observed for the composite with silica without a coupling agent and with silica/SP. In the case of the former composite, one could hypothesize that the acidic silanols react with sulphenamide, leading to substances, such as benzothiazoles, which are more active in sulfur-based cross-linking.[57] Moreover, a larger extent of the filler network can lead to a lower value of ts_1. The lower value of t_{S1} for silica/SP (with respect to silica/TESPT) could also lead to hypothesize a different reactivity of SP with the sulfur-based cross-linking system. The reactivity of SP with sulfur and sulfur-based chemicals is discussed below in the text.

The analysis of the cross-linking network was performed, for silica/TESPT and silica/SP composites, by performing swelling experiments and elaborating the experimental data with the Flory−Rehner equation, eq 3 in the experimental part. Data are shown in Table 8: total concentration of cross-links, as well as mass% of (mono + di-sulfides) and of poly-sulfides.

The lowest cross-linking density was obtained in the case of the composite without the coupling agent, as expected. The total concentration of cross-linking points appears to be similar for the composites containing a coupling agent. Higher values of mono- and di-sulfide were obtained with SP as the silica

https://doi.org/10.1021/acssuschemeng.2c04617
ACS Sustainable Chem. Eng. 2023, 11, 2713−2726

Table 8. Structure of the Cross-Linking Network of Composites of Table 1

	silica	silica/TESPT	silica/SP
total cross-links (mol/g)	1.8	2.4	2.2
mono and di-sulfides (% mass)	46.5	52.4	63.5
poly-sulfides (% mass)	53.5	47.6	36.5

coupling agent. This can justify the higher value of M_H modulus detected with the rheometric experiment and suggests a different mechanism for the cross-linking reaction.

3.3.2. Dynamic–Mechanical Properties. Dynamic–mechanical properties were measured by applying a sinusoidal stress in the axial mode. Details are in the experimental part. The results are shown in Table 9.

Table 9. Results from Dynamic Compression Tests[a] for Composites of Table 1

	silica	silica/TESPT	silica/SP
$E'_{10°C}$	10.35	7.83	9.86
$E'_{23°C}$	7.68	5.86	7.13
$E'_{70°C}$	5.56	4.35	5.15
$\lvert E'_{70°C} - E'_{10°C}\rvert$	4.79	3.3	4.71
tan delta @10 °C	0.63	0.58	0.61
tan delta @23 °C	0.39	0.34	0.38
tan delta @70 °C	0.13	0.10	0.11

[a]Tests performed at 100 Hz.

The graph showing the dependence of E' on the temperature is given in Figure S.4 in the Supporting Information.

The composite with silica without any coupling agent revealed much higher values of E' at all the temperatures and of $(E'_{70°C} - E'_{10°C})$ and higher values of tan delta. These findings are due to the remarkable amount of the filler network, formed by silica without a coupling agent. The silica/SP composite had higher values of E', at all the temperatures, with respect to the silica/TESPT composite, hence higher dynamic rigidity, particularly at low temperatures. This could be ascribed to the lower shielding ability of SP and, in particular, to the larger amount of short sulfur bridges in the cross-linking network.

The values of tan delta are slightly higher for the silica/SP composite, with respect to the silica/TESPT composite.

3.3.3. Tensile Properties. Tensile properties were determined by means of quasi-static measurements. Data are shown in Table 10 and graphs with stresses vs strain are shown in Figure S.5 in the Supporting Information.

The composite without any coupling agent for silica had lower mechanical reinforcement, in particular, lower stress at large deformations and reduced stress at break. The composite with the silica/SP adduct revealed lower stresses for strain larger than 100%, but better ultimate properties, with higher elongation at break and similar stress at break. The tensile properties give a meaningful indication of the interaction between a reinforcing filler and the elastomer matrix. In the case of the silica/SP adduct, the lower values of stresses at 100% and, in particular, at 300% elongation could be thus ascribed to a poorer interaction of the silica/SP adduct with the elastomer chains. In the next two paragraphs, the occurrence of the reactions of model pyrrole compounds with alcoxysilanes and sulfur and sulfur-based compounds as well as the occurrence of the reaction of the sulphurated pyrrole with an alkene are demonstrated. Hence, SP appears to be able to act as the coupling agent. A working hypothesis to explain the results obtained from tensile tests could be based on the reactivity of the pyrrole compound with sulfur: in the text below, the formation of sulfur rings on the pyrrole compound is shown. Hence, SP could behave as a trap of sulfur atoms. To verify such hypothesis, silica-based composites were prepared, with the same recipes shown in Table 1 and with either TESPT or SP as the silica modifier, by using a lower amount of SP in the silica/SP adduct, thus increasing the sulfur/SP ratio. A number of 3.9 parts (parts of SP/100 parts of silica) were in the adduct, instead of 9.6 parts. For the sake of clarity, the recipes are shown in Table S.2 in the Supporting Information. Dynamic–mechanical tests in the axial mode and tensile measurements were performed. Values obtained for the dynamic–mechanical and tensile properties are shown in Tables S.3 and S.4 respectively, in the Supporting Information. The graph showing the dependence of stresses on elongation is shown in Figure 4.

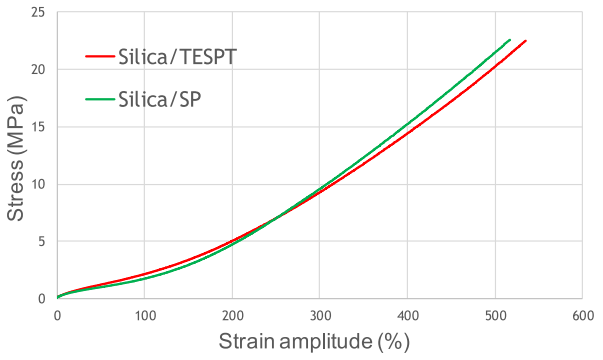

Figure 4. Stress–strain curves from quasi-static measurements on composites of Table 1.

Table 10. Results from Tensile Tests for Composites of Table 1

	silica	silica/TESPT	silica/SP
σ_{50}	1.09	1.02	1.00
σ_{100}	1.52	1.77	1.52
σ_{300}	4.78	9.35	6.03
$\sigma_{300}/\sigma_{100}$	3.14	5.28	3.97
σ_B	16.01	20.59	20.06
ε_B	597.74	492.30	627.90

The values of the dynamic–mechanical properties of the composite with the silica/SP adduct can be explained with the lower amount of SP in the adduct. However, they are not much different from those of the TESPT-based composite. Data in Table S.4 and curves in Figure 4 reveal that the SP and the TESPT-based composites have very similar tensile properties. These findings, obtained in spite of the lower amount of SP in the silica/SP adduct, seem to support the hypothesis of sulfur sequestration by the pyrrole compound.

On the basis of the characterization of the silica-based elastomeric composites, discussed above, it appears that SP acts as a coupling agent for silica. To have silica/SP composite's properties like those of the silica/TESPT-based

https://doi.org/10.1021/acssuschemeng.2c04617
ACS Sustainable Chem. Eng. 2023, 11, 2713–2726

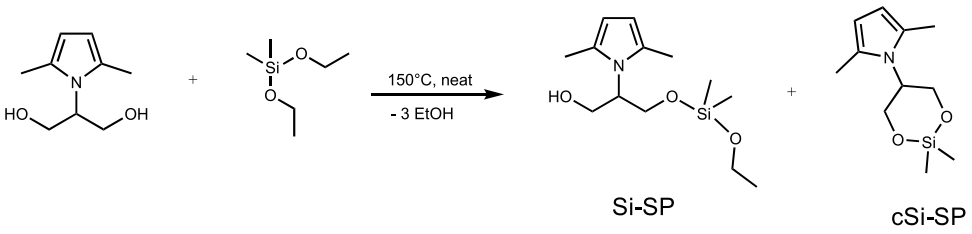

Figure 5. Reaction of SP with diethoxydimethylsilane. Main products are indicated.

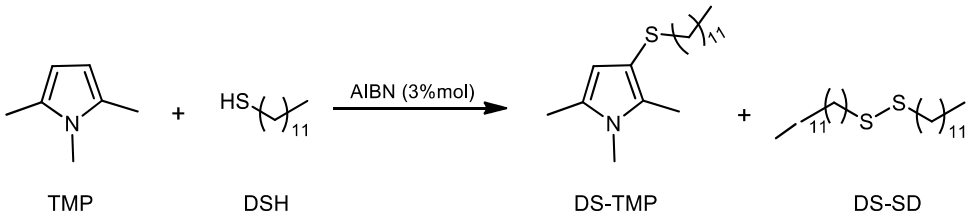

Figure 6. Reaction of trimethylpyrrole with dodecanethiol in the presence of AIBN.

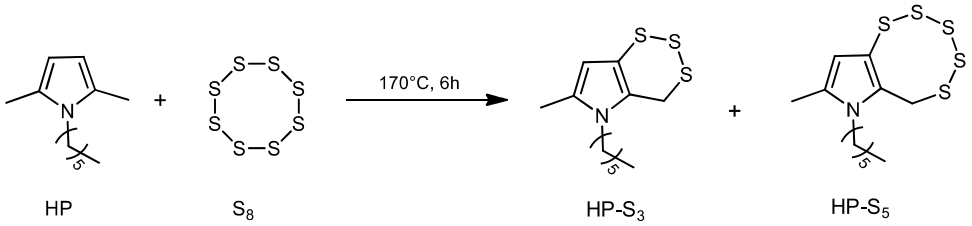

Figure 7. Reaction of hexylpyrrole with S_8.

composite, tuning of the composite formulation must be performed.

3.4. Reaction of SP with an Alkoxysilane. To be a coupling agent, SP should be able to form covalent bonds with silica and with the elastomer chains, by means of sulfur bridges. The reactivity of SP with alcoxysilanes was investigated and is discussed in this paragraph.

A neat reaction was performed between an equimolar amount of SP and diethoxydimethylsilane, as a model compound, as shown in Figure 5. The reaction was performed at 150 °C, for 2 h.

The GC−MS analysis, shown in Figure S.6 in the Supporting Information, revealed the formation of 1-(2,2-dimethyl-1,3,2-dioxasilinan-5-yl)-2,5-dimethyl-1*H*-pyrrole (cSi-SP), as the main product (about 47% yield) and of 2-(2,5-dimethyl-1*H*-pyrrol-1-yl)-3-((ethoxydimethylsilyl)oxy)propan-1-ol (Si-SP) (about 10% yield), besides the unreacted reagents. The formation of spirosilicates from the reaction of silica with the −OH groups of ethylene glycol has been reported.[58]

Moreover, a neat reaction was performed between diethoxydimethylsilane and 2-(2,5-dimethyl-1*H*-pyrrol-1-yl)-ethan-1-ol (ethanol pyrrole, EP), by adopting the same experimental conditions. The scheme of the reaction is shown in Figure S.7 in the Supporting Information. The ^{1}H-NMR spectrum of the reaction product, in Figure S.8 in the Supporting Information, revealed the presence of 1-(2-((ethoxydimethylsilyl)oxy)ethyl)-2,5-dimethyl-1*H*-pyrrole (Si-EP) and bis-(2-(2,5-dimethyl-1*H*-pyrrol-1-yl)ethoxy)-dimethylsilane (Si-bisEP), which means the mono- and the di-condensation products.

These findings indicate that a pyrrole compound with OH groups, in the group substituent of the nitrogen atom, e.g., SP, can react with an alcoxysilane, at the temperature used for the processing of the elastomer composite and for a time much longer than the one adopted for a tire compound processing, without degradation of the pyrrole ring.

3.5. Reaction of a Pyrrole Compound with Sulfur and Sulfur-Based Chemicals and of the Sulfurated Pyrrole Compound with Squalene. The reactivity of model pyrrole compounds with sulfur and sulfur-based chemicals was studied. Then, it was investigated the reactivity of the sulphurated pyrrole compound with a model unsaturated hydrocarbon.

3.5.1. Reaction of Pyrrole Compounds with Dodecanthiol and with Sulfur. A reaction was performed between 1,2,5-trimethyl-1*H*-pyrrole, as a model compound, and dodecanethiol in the presence of 2−2′-azaisobutyronitrile as the radical initiator, as shown in Figure 6. Details are in the experimental part. In brief, TMP was dissolved at 75 °C in an excess of dodecanethiol, under nitrogen. After 1 h, AIBN (3% mol with respect to TMP) was added and the reaction mixture was left under stirring until the disappearance of TMP checked by means of TLC. After 12 h, the reaction was stopped just by evaporating the reagents under reduced pressure.

The GC−MS chromatograph is shown in Figure S.9 in the Supporting Information.

The GC−MS analysis revealed the presence of two main products: 3-(dodecylthio)-1,2,5-trimethyl-1*H*-pyrrole (DS-TMP) and the dimer of dodecanethiol, 1,2-didodecyldisulfane (DS-SD). It is worth observing that only the mono-addition of thiol to the pyrrole ring was documented.

A neat reaction was performed between 1-hexyl-2,5-dimethyl-1*H*-pyrrole (hexylpyrrole, HP) and orthorhombic sulfur, as shown in Figure 7. Details are in the experimental

https://doi.org/10.1021/acssuschemeng.2c04617
ACS Sustainable Chem. Eng. 2023, 11, 2713−2726

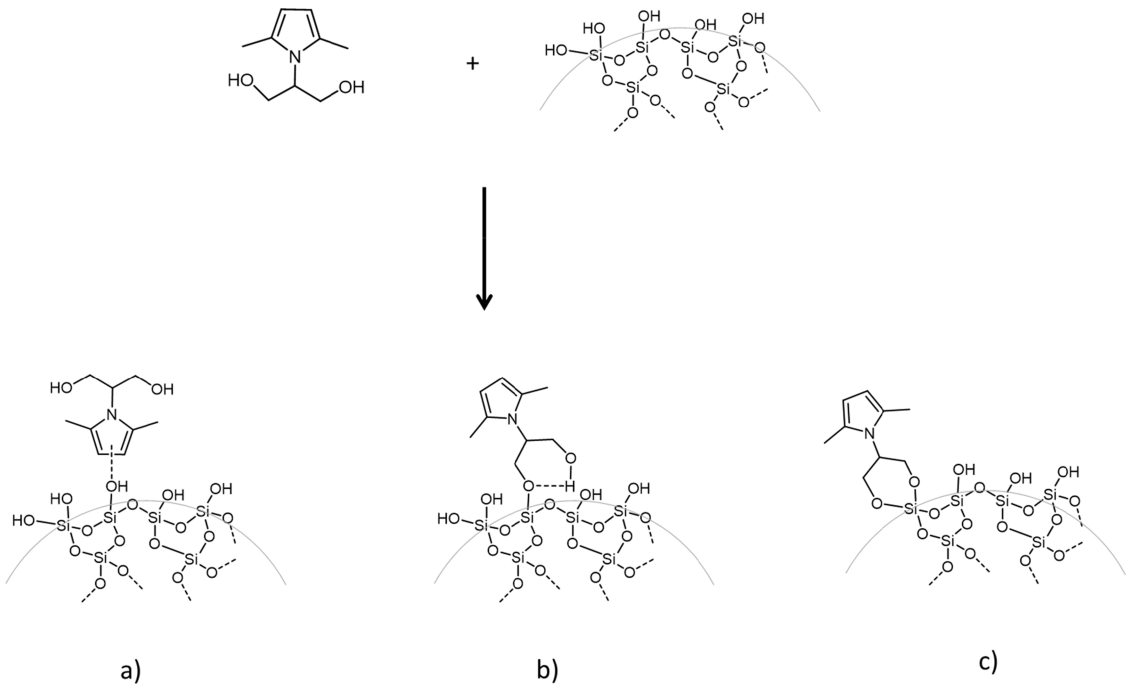

Figure 8. Hypothesis of mechanism for the formation of the silica/SP adduct.

part. In brief: the reaction was carried out under nitrogen, for 6 h, at 170 °C, which was the cross-linking temperature.

The reaction mixture was checked by means of GC−MS. The GC−MS chromatogram, shown in Figure S.10 in the Supporting Information, revealed the presence, besides the unreacted TMP, of two reaction products, whose molecular mass could be justified with the chemical structures of HP-S_3 and HP-S_5, as shown in Figure 7. Sulfur rings are formed between the alpha methyl and the beta position of the pyrrole ring.

The findings reported above indicate that the pyrrole compound is able to react with sulfur and with a thiyl radical at the temperature typical of the cross-linking reaction of the elastomeric composite. In particular, the reaction with the thiyl radical could account for the short induction time of cross-linking. In fact, it is known[57] that in the first time of a sulfur-based cross-linking, the radical mechanism occurs more than the concerted one, based on the active sulfurating species, which takes time to be formed.

3.5.2. Reaction of Sulfurated Pyrrole Compounds with an Alkene. To investigate the occurrence of the reaction between the unsaturated elastomer and the sulfurated pyrrole compound, whose formation has been demonstrated and discussed in the previous paragraph, a reaction was performed between the sulfurated pyrrole compound and squalene, selected as the model compound for the unsaturated elastomer. Trimethylpyrrole was selected as the pyrrole compound. Details are in the experimental part. The reaction product was analyzed by means of ^{13}C-NMR. The ^{13}C-NMR spectra of squalene and of the reaction mixture are shown in Figure S.11 in the Supporting Information. Three types of C=C double bonds are present in the squalene molecule. They gave rise to six peaks in the NMR spectrum, which were taken as markers of the reaction with the sulphurated pyrrole ring. In the spectrum of the reaction product, these peaks were split, and peaks at higher fields were clearly visible,[59] to indicate the occurrence of the reaction of sulfur with allylic hydrogen. On the basis of the relative intensity of the peaks, the C6 and C10 positions appear to be the most reactive one.

3.6. Hypothesis of the Mechanism for the Formation of the Silica/Unsaturated Elastomer Bond with SP as the Coupling Agent. On the basis of the results reported in Paragraph 3.4, a hypothesis of mechanism was elaborated for the formation of the silica/SP adduct. As shown in Figure 8, the silica/SP adduct could be formed through a supramolecular interaction (a) and via the condensation of silanols with one (b) or two (c) OH groups of SP.

Taking into consideration the stable interaction of SP with silica, shown by the results of acetone extraction and by the composites' properties, the formation of covalent bonds should be the preferred hypothesis and, in the light of what reported in the scientific literature on the silanols' reactivity, the condensation of only one OH group could preferentially occur. At the present stage of the research, this appears to be the most reasonable hypothesis. However, further experiments are in progress, taking also into consideration the reactivity of the pyrrole ring.

On the basis of the results reported in Paragraph 3.5, it appears reasonable to assume that a sulphurated pyrrole ring is able to react with the allylic positions of the unsaturated elastomer.

The picture of the silica-elastomer bond mediated by SP as the coupling agent is shown in Figure 9.

4. CONCLUSIONS

A biosourced *Janus* molecule, such as SP, is indeed a coupling agent between silica and an unsaturated elastomer, such as natural rubber and SBR, in a sulfur-cured elastomer composite suitable for tire compounds. The whole process which leads to the formation of the silica/SP adduct can be performed by using biosourced chemicals, in the absence of solvents and catalysts, with water as the only co-product and with carbon efficiency close to 100%. The use of SP as the silica coupling agent allows to avoid ethanol emission, typical of the silica

https://doi.org/10.1021/acssuschemeng.2c04617
ACS Sustainable Chem. Eng. 2023, 11, 2713−2726

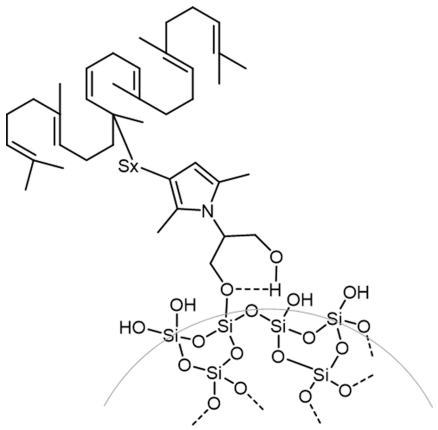

Figure 9. Picture of the silica-elastomer bond with SP as the coupling agent.

silanization reaction with TESPT. By considering equal to 1:1, the (released ethanol/Si atom in TESPT) molar ratio, the values for the global production of tires,[8] reported in the Introduction, the mass of a tire (10 kg), the mass of a tire tread and of silica in the tire tread (35% in both cases), the mass% of TESPT with respect to silica (8%), and taking also into account that the released ethanol is burned, it can be calculated that 8.44×10^4 tonnes of CO_2 are released in one year as a consequence of the use of TESPT in a tire tread. Similar dynamic−mechanical properties can be obtained for SP- and TESPT-based composites. It is worth underlining the similar value of tan delta, which is taken in the tire field as the index of the hysteresis of a tread compound, which in turn leads to the RR of a tire. These results can be explained on the basis of the formation of covalent bonds: between the PyC and silica, through the condensation of OH and SiOH groups, between the PyC and sulfur and between the sulphurated PyC and the unsaturated elastomer chains. The synthesis of SP is indeed a simple reaction and can be performed on silica. The preparation of the adduct in situ, during the elastomer composite preparation, could reasonably be envisaged. Hence, the results here reported could pave the way for a large-scale development, with a remarkable reduction of the carbon footprint of tire technology. Other compounds containing a pyrrole moiety could be prepared, giving rise to a family of *Janus* molecules.

To the best of our knowledge, a biosourced coupling agent for silica, with such high efficiency for silica functionalization, suitable for the scale up to the industrial scale, has never been reported. The development of this technology[60] to the industrial scale has been recently announced by a major player in the tire field.[61] SP appears to be a reasonable alternative to the silane TESPT, through the development of an ad hoc formulation of the composite. The research should be aimed at promoting reduction of the hysteresis of the compound and, consequently, of the rolling resistance of a tire. The impact of RR on the fuel economy is estimated with the so-called Return Factor, the ratio between the change (%) in fuel consumption to the corresponding change (%) in rolling resistance.[10] For modern passenger cars, the Return Factor is estimated to be between 0.5:10 and 1.5:10.[10] By considering that the fuel consumption in USA was of about 723,665 million liters in 2020[62] and by assuming a Return Factor of 0.15, a reduction of rolling resistance of 20% would lead to a fuel saving of about 3%, which corresponds to 21,710 million liters. Taking into consideration that the CO_2 emission is 1.93 (kg/L of motor gasoline),[63] the reduction of CO_2 emission is of about 42 million ton. Further tuning is indeed possible, for example, by selecting the appropriate ingredients of the elastomer composite, namely, the components of the cross-linking system.[64]

Pyrrole compounds were shown able to form adducts with sp^2 carbon allotropes[39,40] and to act as coupling agents for carbon black in elastomeric composites. Hence, they appear to be suitable as universal coupling agents with both inorganic oxides-hydroxides and sp^2 carbon allotropes.

■ ASSOCIATED CONTENT

Supporting Information

The Supporting Information is available free of charge at https://pubs.acs.org/doi/10.1021/acssuschemeng.2c04617.

C and N contents in silica/SP adducts (Table S.1); FT-IR spectra of silica/SP physical mixtures (Figure S.1); silica/SP adducts obtained by performing the synthesis of SP on silica (Figure S.2); GC−MS chromatograms of the reaction the reaction of SP with dietoxydimethylsilane (Figure S.6); ^{1}H NMR spectra of the reaction products of the reaction shown in Figure S.6 (Figure S.8.); ^{13}C NMR spectra of squalene and of the reaction mixture obtained by reacting the sulfurated trimethylpyrrole and squalene (Figure S.11.); formulations of silica-based composites with different coupling agents for silica (Table S.2); results from dynamic compression tests for composites of Table S.2 (Table S.3); and results from tensile tests for composites of Table S.2 (Table S.4) (PDF)

■ AUTHOR INFORMATION

Corresponding Authors

Vincenzina Barbera − *Department of Chemistry, Materials and Chemical Engineering "G. Natta", Politecnico di Milano, Milano 20131, Italy*; orcid.org/0000-0002-4503-4250; Email: vincenzina.barbera@polimi.it

Maurizio Galimberti − *Department of Chemistry, Materials and Chemical Engineering "G. Natta", Politecnico di Milano, Milano 20131, Italy*; orcid.org/0000-0001-5770-7208; Email: maurizio.galimberti@polimi.it

Authors

Daniele Locatelli − *Department of Chemistry, Materials and Chemical Engineering "G. Natta", Politecnico di Milano, Milano 20131, Italy*

Andrea Bernardi − *Department of Chemistry, Materials and Chemical Engineering "G. Natta", Politecnico di Milano, Milano 20131, Italy*

Lucia Rita Rubino − *Department of Chemistry, Materials and Chemical Engineering "G. Natta", Politecnico di Milano, Milano 20131, Italy*

Stefania Gallo − *Department of Chemistry, Materials and Chemical Engineering "G. Natta", Politecnico di Milano, Milano 20131, Italy*

Alessandra Vitale − *Department of Applied Science and Technology, Politecnico di Torino, Torino 10129, Italy*; orcid.org/0000-0002-8682-3125

Roberta Bongiovanni − *Department of Applied Science and Technology, Politecnico di Torino, Torino 10129, Italy*; orcid.org/0000-0002-2607-9461

Complete contact information is available at:
https://pubs.acs.org/10.1021/acssuschemeng.2c04617

Notes

The authors declare no competing financial interest.

■ ACKNOWLEDGMENTS

This work was financially supported by Pirelli Tyre.

■ REFERENCES

(1) To meet the needs of the present without compromising the ability of future generations to meet their own needs. *Our Common Future*; Oxford University Press: U.S.A., 1990, 27
(2) Allen, D. T.; Hwang, B. J.; Licence, P.; Pradeep, T.; Subramaniam, B. Advancing the use of sustainability metrics. *ACS Sustainable Chem. Eng.* **2018**, 3102359−3102360.
(3) https://www.epa.gov/sustainability. Access 27th July 2022
(4) https://www.worldtop20.org/ Access: 27th July 2022
(5) https://www.un.org/sustainabledevelopment/development-agenda/. Access the 27thJuly 2022
(6) *Our world in data.org. research and data to make progress against the world's largest problems*; Source: Climate Watch, the World resource Institute (2020).
(7) *Global Mobility Report 2017, Tracking Sector Performance. Sustainable mobility for all*. 2017.
(8) https://www.reportlinker.com/p05379599/?utm_source=GNW. Access: 27th July 2022.
(9) Pirelli Tyre*Global High Value − Company presentation − November 2019*. 2019
(10) Hall, D. E.; Moreland, J. C. Fundamentals of Rolling Resistance. *Rubber Chem. Technol.* **2001**, *74*, 525−539.
(11) Chevalier, Y.; Morawski, J.C.Precipitated silica with morphological properties, process for producing it and its application, especially as a filler. Legrand EP0157703 B1. Priority: 1984.04.06
(12) Legrand, A.P.; On the silica edge. In: Legrand, A.P. (Ed.), *The surface properties of silicas*; Wiley and Sons New York, 1998, 1−20
(13) Leblanc, J. L. Rubber-filler interactions and rheological properties in filled compounds. *Prog. Polym. Sci.* **2002**, *27*, 627−687.
(14) Donnet, J.B.; Custodero, E.Reinforcement of Elastomers by Particulate Fillers. In: Mark, J.E., Erman, B., Eirich, F.R. (Eds.) *The Science and Technology of Rubber Third Ed.*; Academic Press2005, 367−400.
(15) Fröhlich, J.; Niedermeier, W.; Luginsland, H. D. The effect of filler-filler and filler-elastomer interaction on rubber reinforcement. *Compos. Part A Appl. Sci. Manuf.* **2005**, *36*, 449−460.
(16) Hayichelaeh, C.; Reuvekamp, L. A. E. M.; Dierkes, W. K.; Blume, A.; Noordermeer, J. W. M.; Sahakaro, K. Enhancing the Silanization Reaction of the Silica-Silane System by Different Amines in Model and Practical Silica-Filled Natural Rubber Compounds. *Polymers (Basel)* **2018**, *10*, 584.
(17) Blume, A.; Janik, M.; Gallas, P.; Thibault-Starzyk, F.; Vimont, A. Operando infrared study of the reaction of triethoxypropylsilane with silica. *KGK Kautsch. Gummi Kunstst.* **2008**, *61*, 359−362.
(18) Sheldon, R. A. Green and sustainable manufacture of chemicals from biomass: state of the art. *Green Chem.* **2014**, *16*, 950−963.
(19) Varma, R. S. Biomass-derived renewable carbonaceous materials for sustainable chemical and environmental applications. *ACS Sustainable Chem. Eng.* **2019**, *7*, 6458−6470.
(20) Anastas, P. T.; Warner, J. C.; *Green chemistry: theory and practice*; Oxford University Press, 2000
(21) Sheldon, R. A. Metrics of green chemistry and sustainability: past, present, and future. *ACS Sustainable Chem. Eng.* **2018**, *6*, 32−48.
(22) Barbera, V.; Citterio, A.; Galimberti, M.; Leonardi, G.; Sebastiano, R.; Shisodia, S. U.; Valerio, A.M.; Process for the synthesis of 2-(2,5-dimethyl-1H-pyrrol-1-yl)-1,3-propanediol and its substituted derivativesUS 10329253 B22019
(23) Knorr, L. Einwirkung des Diacetbernsteinsäureesters auf Ammoniak und primäre Aminbasen. *Chem. Ber.* **1885**, *18*, 299.
(24) Paal, C. Synthese von Thiophen-und Pyrrolderivaten. *Chem. Ber.* **1885**, *18*, 2251−2254.
(25) Yang, F.; Hanna, M. A.; Sun, R. Value-added uses for crude glycerol − a by-product of biodiesel production. *Biotechnol. Biofuels* **2012**, *5*, 13.
(26) Werpy, T.; Petersen, G.; *TopValueAddedChemicals fromBiomass. Volume I - Results of Screening for Potential Candidates from Sugars and Synthesis Gas*; U. S. D. o. Energy2004
(27) Joseph, J.; Bozell, R.; Petersen, G. R. Technology development for the production of biobased products from biorefinery carbohydrates. *Green Chem.* **2010**, *12*, 539−554.
(28) Jérôme, F.; Pouilloux, Y.; Barrault, J. Rational design of solid catalysts for the selective use of glycerol as a natural organic building block. *ChemSusChem.* **2008**, *1*, 586−613.
(29) Andreeßen, B.; Steinbüchel, A. Serinol: small molecule - big impact. *AMB Express* **2011**, *1*, 12.
(30) Kuhlmann, B.; Arnett, E. M.; Siskin, M. Classical organic reactions in pure superheated water. *J. Org. Chem.* **1994**, *59*, 3098−3101.
(31) Zhang, Y.; Li, W.; Zong, S.; Du, H.; Shi, X. Continuous synthesis of 2, 5-hexanedione through direct C−C coupling of acetone in a Hilbert fractal photo microreactor. *Adv. Mater. Res.* **2012**, *518-523*, 3947−3950.
(32) Li, Y.; Lv, G.; Wang, Y.; Deng, T.; Wang, T.; Hou, X.; Yang, Y. Synthesis of 2, 5-Hexanedione from Biomass Resources Using a Highly Efficient Biphasic System. *ChemistrySelect* **2016**, *1*, 1252−1255.
(33) de Gennes, P. G. Soft matter (nobel lecture). *Angew. Chem., Int. Ed.* **1992**, *31*, 842−845.
(34) Galimberti, M.; Barbera, V.; Guerra, S.; Conzatti, L.; Castiglioni, C.; Brambilla, L.; Serafini, A. Biobased Janus molecule for the facile preparation of water solutions of few layer graphene sheets. *RSC Adv.* **2015**, *5*, 81142−81152.
(35) Brambila, C.; Boyd, P.; Keegan, A.; Sharma, P.; Vetter, C.; Ponnusamy, E.; Patwardhan, S. V. A comparison of environmental impact of various silicas using a green chemistry evaluator. *ACS Sustainable Chem. Eng.* **2022**, *10*, 5288−5298.
(36) Feng, J. X.; Xu, H.; Ye, S. H.; Ouyang, G.; Tong, Y. X.; Li, G. R. Silica−Polypyrrole Hybrids as High-Performance Metal-Free Electrocatalysts for the Hydrogen Evolution Reaction in Neutral Media. *Angew. Chem., Int. Ed.* **2017**, *129*, 8232−8236.
(37) Wu, F.; Sun, M.; Chen, C.; Zhou, T.; Xia, Y.; Xie, A.; Shang, Y. Controllable coating of polypyrrole on silicon carbide nanowires as a core−shell nanostructure: a facile method to enhance attenuation characteristics against electromagnetic radiation. *ACS Sustainable Chem. Eng.* **2019**, *7*, 2100−2106.
(38) Pourabbas, B.; Pilati, F. Polypyrrole grafting onto the surface of pyrrole-modified silica nanoparticles prepared by one-step synthesis. *Synth. Met.* **2010**, *160*, 1442−1448.
(39) Locatelli, D.; Barbera, V.; Brambilla, L.; Castiglioni, C.; Sironi, A.; Galimberti, M. Tuning the Solubility Parameters of Carbon Nanotubes by Means of Their Adducts with Janus Pyrrole Compounds. *Nanomaterials* **2020**, *10*, 1176.
(40) Galimberti, M.; Barbera, V.; Guerra, S.; Bernardi, A. Facile functionalization of sp^2 carbon allotropes with a biobased Janus molecule. *Rubber Chem. Technol.* **2017**, *90*, 285−307.
(41) Musto, S.; Barbera, V.; Cipolletti, V.; Citterio, A.; Galimberti, M. Master curves for the sulphur assisted crosslinking reaction of natural rubber in the presence of nano-and nano-structured sp^2 carbon allotropes. *Express Polym. Lett.* **2017**, *11*, 435−448.
(42) Barbera, V.; Leonardi, G.; Valerio, A.; Rubino, L.; Sun, S.; Famulari, A.; Galimberti, M.; Citterio, A.; Sebastiano, R. Environmentally Friendly and Regioselective One-Pot Synthesis of Imines and Oxazolidines Serinol Derivatives and Their Use for Rubber Cross-Linking. *ACS Sustainable Chem. Eng.* **2020**, *8*, 9356−9366.
(43) McCabe, W. L., Smith, J. C., Harriott, P., *Unit Operations of Chemical Engineering*7th edition; McGraw-Hill Education, 2004, 824−826, ISBN 9780071247108

(44) Matsumoto, A.; Tsutsumi, K.; Schumacher, K.; Unger, K. K. Surface functionalization and stabilization of mesoporous silica spheres by silanization and their adsorption characteristics. *Langmuir* **2002**, *18*, 4014−4019.
(45) Krasnoslobodtsev, A. V.; Smirnov, S. N. Effect of water on silanization of silica by trimethoxysilanes. *Langmuir* **2002**, *18*, 3181−3184.
(46) Thibault-Starzyk, F.; Gil, B.; Aiello, S.; Chevreau, T.; Gilson, J. P. In situ thermogravimetry in an infrared spectrometer: An answer to quantitative spectroscopy of adsorbed species on heterogeneous catalysts. *Microporous Mesoporous Mater.* **2004**, *67*, 107−112.
(47) Hartmeyer, G.; Marichal, C.; Lebeau, B.; Rigolet, S.; Caullet, P.; Hernandez, J. Speciation of silanol groups in precipitated silica nanoparticles by 1H MAS NMR spectroscopy. *J. Phys. Chem. C* **2007**, *111*, 9066−9071.
(48) Gallas, J. P.; Goupil, J. M.; Vimont, A.; Lavalley, J. C.; Gil, B.; Gilson, J. P.; Miserque, O. Quantification of water and silanol species on various silicas by coupling IR spectroscopy and in-situ thermogravimetry. *Langmuir* **2009**, *25*, 5825−5834.
(49) Golubeva, O. Y.; Maslennikova, T. P.; Ulyanova, N. Y.; Dyakina, M. P. Sorption of lead(II) ions and water vapors by synthetic hydro- and aluminosilicates with layered, framework, and nanotube morphology. *Glass Phys. Chem.* **2014**, *40*, 250−255.
(50) Zhang, C.; Tang, Z.; Guo, B.; Zhang, L. Significantly improved rubber-silica interface via subtly controlling surface chemistry of silica. *Compos. Sci. Technol.* **2018**, *156*, 70−77.
(51) Blume, A.; Jin, J.; Mahtabani, A.; He, X.; Kim, S.; Andrzejewska, Z. J.; New Structure Proposal for Silane Modified Silica. *Paper presented at International Rubber Conference*; IRC 2019: London, United Kingdom2019.
(52) Beganskiene, A.; Sirutkaitis, V.; Kurtinaitiene, M.; Juskenas, R.; Kareiva, A. FTIR, TEM and NMR Investigations of Stober Silica Nanoparticles. *Mater. Sci.* **2004**, *10*, 287−290. ISSN 1392−1320
(53) Marrone, M.; Montanari, T.; Busca, G.; Conzatti, L.; Costa, G.; Castellano, M.; Turturro, A. A Fourier transform infrared (FTIR) study of the reaction of triethoxysilane (TES) and bis [3-triethoxysilylpropyl] tetrasulfane (TESPT) with the surface of amorphous silica. *J. Phys. Chem. B* **2004**, *108*, 3563−3572.
(54) Kallury, K. M. R.; Macdonald, P. M.; Thompson, M. Effect of Surface Water and Base Catalysis on the Silanization of Silica by (Aminopropyl) alkoxysilanes Studied by X-ray Photoelectron Spectroscopy and 13C Cross-Polarization/Magic Angle Spinning Nuclear Magnetic Resonance. *Langmuir* **1994**, *10*, 492−499.
(55) Sosa, N.; Chanlek, N.; Wittayakun, J. Facile ultrasound-assisted grafting of silica gel by aminopropyltriethoxysilane for aldol condensation of furfural and acetone. *Ultrason. Sonochem.* **2020**, *62*, No. 104857.
(56) Szili, E. J.; Kumar, S.; Smart, R. S. C.; Voelcker, N. H. Generation of a stable surface concentration of amino groups on silica coated onto titanium substrates by the plasma enhanced chemical vapour deposition method. *Appl. Surf. Sci.* **2009**, *255*, 6846−6850.
(57) Coran, A.Y.; in *The Science and Technology of Rubber Third Ed.* Eds.; Elsevier Academic Press2005, *7*, 321−366
(58) Jitchum, V.; Chivin, S.; Wongkasemjit, S.; Ishida, H. Synthesis of spirosilicates directly from silica and ethylene glycol/ethylene glycol derivatives. *Tetrahedron* **2001**, *57*, 3997−4003.
(59) Barbarella, G.; Dembech, P.; Garbesi, A.; Fava, A. 13C NMR of organosulphur compounds: I—the effects of sulphur substituents on the 13C chemical shifts of alkyl chains and of S-heterocycles. *Org. Magn. Reson.* **1976**, *8*, 108−114.
(60) Galimberti, M; Bernardi, A.; Barbera, V.; Locatelli, DAdduct between a pyrrolic compound and an inorganic oxide hydroxide, a super-adduct between a pyrrolic compound, an inorganic oxide hydroxide and a carbon allotrope, elastomeric composition comprising the super-adduct and methods for producing the sameWO2019/162873. Priority 2018.02.21
(61) https://www.bts.gov/content/motor-vehicle-fuel-consumption-and-travel. Access the 4th October 2022.
(62) Pirelli Tyre; *Annual Report: The Human Dimension*. 2020, 106.
(63) https://corporate.pirelli.com/var/files2020/EN/PDF/PIRELLI_ANNUAL_REPORT_2020_ENG.pdf Access the 4th October 2022.
(64) https://www.eia.gov/environment/emissions/co2_vol_mass.php. Access the 4th October 2022.

NOTE ADDED AFTER ASAP PUBLICATION

This paper posted ASAP on February 6, 2023, with an error in the TOC/Abstract. The corrected version was reposted on February 8, 2023.